HHS Public Access

Author manuscript

Behav Brain Res. Author manuscript; available in PMC 2019 July 02.

Published in final edited form as:

Behav Brain Res. 2018 July 02; 346: 21–28. doi:10.1016/j.bbr.2017.12.008.

Changes in cognition and dendritic complexity following intrathecal Methotrexate and Cytarabine treatment in a juvenile murine model

Tyler C. Alexander[a,b], **Christy M. Simecka**[d], **Frederico Kiffer**[a,b], **Thomas Groves**[a,b,c], **Julie Anderson**[a,b], **Hannah Carr**[a], **Jing Wang**[a,b], **Gwendolyn Carter**[a,b], and **Antiño R. Allen**[a,b,c,*]

[a]Division of Radiation Health, University of Arkansas for Medical Sciences, Little Rock, AR 72205, USA

[b]Department of Pharmaceutical Sciences, University of Arkansas for Medical Sciences, Little Rock, AR, 72205, USA

[c]Department of Neurobiology & Developmental Sciences, University of Arkansas for Medical Sciences, Little Rock, AR 72205, USA

[d]Division of Laboratory Animal Medicine, University of Arkansas for Medical Sciences, Little Rock, Arkansas 72205, USA

Abstract

Acute lymphoblastic leukemia (ALL) is the most prevalent childhood cancer and accounts for 26.8% of cancer diagnoses among children, worldwide—approximately 3,000 children each year. While advancements in treating ALL have led to a remission rate of more than 90%, many survivors experience adverse neurocognitive and/or neurobehavioral effects as a result of intrathecal chemotherapy. Methotrexate (MTX) is commonly administered with cytosine arabinoside (AraC, cytarabine) during intrathecal chemotherapy for ALL. To date, few studies exist that test the cognitive effects of intrathecal injections of MTX/AraC on juvenile populations. The purpose of our study was to investigate the combined effects of MTX/AraC on cognition and dendritic structure in the hippocampus in juvenile male mice. Twenty, 21-day-old male C57BL/6 mice were used in this study; 10 mice received intrathecal MTX/AraC treatment, and 10 were given intrathecal saline injections. Five weeks after injections, we tested the animals' hippocampus-dependent cognitive performance in the Morris water maze. After the first day of hidden-platform training, we observed that the mice that received MTX/AraC treatment showed signs of significant impairment in spatial memory retention. MTX/AraC treatment significantly compromised the dendritic architecture and reduced mushroom spine density in the dorsal ganglion (DG), CA1, and CA3 areas of the hippocampus. The present data provided evidence that MTX/AraC compromised the dendritic architecture and impaired hippocampal dependent

*Address for corresponding author: Antiño R. Allen, University of Arkansas for Medical Sciences, 4301 W. Markham 441B-2, Little Rock, AR 72205, Phone: 501-686-7553; fax: 501-526-6599; AAllen@uams.edu.

cognition. This could provide insight into chemotherapy-induced cognitive decline in juvenile patients treated for ALL.

Keywords

Chemotherapy; cognitive; dendritic; hippocampus; impairment; morphology

1. INTRODUCTION

In the past 50 years, the survival rate for acute lymphoblastic leukemia (ALL) has risen from 10% to 90%, stemming from the use of chemotherapy, radiation, and central nervous system (CNS)-directed therapies.[1–4] In addition, antibiotic and blood product support introduced in the ‘60s and ‘70s greatly improved outcomes.[5] Though ALL treatment protocols vary greatly among clinicians, most therapies consist of a three-part paradigm, which includes induction, consolidation, and maintenance.[6] The goal of induction is to induce remission and restore hematopoiesis, while consolidation is meant to reduce the tumor burden further. Finally, maintenance aims to prevent relapse, and may last for two years, post consolidation. [7] Protocols typically involve some systemic chemotherapy and central nervous system (CNS) directed therapy that consists of intrathecal methotrexate (MTX), cytosine Arabinoside (AraC), and sometimes cranial irradiation.7[i]

Methotrexate (MTX) is commonly used in the maintenance phase of the ALL treatment protocol. The main mechanism of action of MTX is the inhibition of the enzyme dihydrofolate reductase (DHFR). Since DHFR is necessary for the formation of intracellular folates, reduced DHFR activity leads to decreased production of the purines and pyrimidines that are necessary for DNA replication and cell division.[8] Unfortunately, MTX is associated with intense neurotoxicity, especially in CNS-directed therapies; this can result in seizures, occlusive vascular-like events. These MTX-induced toxicities happen acutely and do resolve over time.[9] Damage to the CNS can result in long-term deficits in cognition.[10]

The chemotherapy drug cytosine arabinoside (AraC) is commonly used in ALL treatment, and is often given through an intrathecal injection in conjunction with MTX. Highly effective at preventing DNA synthesis, AraC is a viable treatment for cancer,[11] and more specifically the treatment of tumors, as it effectively reduces tumor size.[12] Cytosine arabinoside (AraC) prevents cells from moving beyond the S-phase of mitosis, making it a potent cell-cycle arrest molecule.[13] With a well-defined mechanism of action, AraC is incorporated into the cellular DNA as a cystine analogue, but because it contains an extra hydroxyl group at the 2’ position of the β configuration, it does not allow for proper DNA or RNA synthesis. This leads to cell-cycle arrest and ultimately apoptosis.[14] Unfortunately, AraC’s functional inhibition of cell-cycle arrest affects all dividing cells, not just cancerous ones. AraC can prevent the formation of new neurons, as neurogenesis continues into adulthood, leading to neurotoxicity and deficits in cognition. In the CNS, AraC has been

[i]Abbreviations: ALL: acute lymphoblastic leukemia; AraC: cytosine Arabinoside; BrdU: bromodeoxyuridine; CNS: central nervous system; DG: Dorsal Ganglion; DHFR: dihydrofolate reductase; *IP: intraperitoneal;* LSD: Fisher’s least significant difference; *MTX: methotrexate;* MWM: Morris water maze; NOR: *novel object recognition;* SEM: Standard Error of the Mean

associated with encephalopathy, seizures, cerebellar syndrome, and cranial neuropathy.[14] These toxicities, especially cranial neuropathy, may lead to post-treatment cognitive dysfunction.

Often referred to as “chemobrain”, chemotherapy-induced cognitive deficits can last for years after treatment.[15] Chemobrain causes impairments in memory, learning, concentration, reasoning, executive function, attention, and visuospatial skills.[16] The cognitive effects of chemotherapy apply to children, as well. Studies of pediatric patients treated for ALL show that many experience cognitive dysfunction after treatment.[17,18] CNS toxicity is inevitable as chemotherapy is injected directly into the spinal fluid, and these therapies are closely associated with a decrease in IQ score that can be rather significant. Pediatric patients affected with chemobrain have IQ scores that are at least one standard deviation below the mean of other children their age.[19]

Very few studies have been published that examine the effects of ALL treatment utilizing a juvenile murine model. The most prominent study was conducted in 2013 by Bisen-Hersh et al. In the study, MTX and AraC were given intraperitoneally to pre-weanling pups. The team then conducted a novel object-recognition task to measure short-term memory, and a conditional-discrimination task to measure mental flexibility. The results showed that the mice that had received MTX alone or MTX in conjunction with AraC performed less well on behavioral tasks when compared to the non-treatment cohort.[20] Unfortunately, the study did not investigate physiological changes that could have confirmed the behavioral results, such as molecular assays. Assessment of neurophysiology could be beneficial in understanding mechanistic changes that lead to damage. Since much of the retention and consolidation of memory is localized to the hippocampus, evaluation of damage to this brain region and interruptions in connectivity could provide insight into the detrimental effects of chemotherapy.[21–23] Therefore, more murine models are needed to study possible mechanisms underlying cognitive decline in juvenile ALL treatment, as well as changes in hippocampal physiology. Furthermore, their study used an intraperitoneal injection method to administer the therapy. In humans, the treatment protocol for ALL involves administration of the drug directly into the spinal canal via intrathecal injection. It is logical that administration of a therapy directly into the CNS would illicit different effects than administration of the same therapy into the abdominal cavity. Intrathecal administration of chemotherapy is more clinically relevant for ALL treatment, models of this treatment paradigm should explore this method.

Therefore, we aimed to not only address the gap in knowledge regarding cognitive decline in pediatric patients, but to provide greater insight into the physiological changes and therapy-induced cognitive decline that accompany intrathecal MTX and AraC therapy, through the use of protocols similar to those used in humans. To accomplish our aims, we developed a study to measure the effects of MTX and AraC on cognition and hippocampal physiology in juvenile mice. We further supported our findings with molecular assays that allow a more thorough understanding of the effects of intrathecal chemotherapy.

1. MATERIALS AND METHODS

2.1 Animals

Male C57BL/6 mice (Jackson Laboratory, Bar Harbor, ME), 21 days old (n = 20), were used in this study. The mice were housed under a constant 12-hour light/12-hour dark cycle and were cared for in compliance with the University of Arkansas for Medical Sciences' (UAMS) Institutional Animal Care and Use Committee.

2.2 Chemotherapy Injections

We administered either 5 mg/kg AraC combined with 10 mg/kg MTX (n=10), or 0.1% saline (n=10) to the mice intrathecally, between the L5 and L6 vertebrae. Once a week for three weeks, each mouse received three injections of either MTX+AraC or saline. Following the chemotherapy injections, we administered five injections of bromodeoxyuridine (BrdU) (10 mg/kg) to each mouse. We then conducted behavioral testing using the Morris water maze (MWM) four weeks after the final BrdU injection.

2.3 Morris Water Maze (MWM)

We assessed hippocampus-dependent cognitive performance 60 days after initiation of chemotherapy administration. To determine if radiation affected the ability of mice to swim or learn the water maze task, a circular pool (diameter, 140 cm) was filled with opaque water (24°C) and the mice were trained to locate a visible platform (luminescence, 200 lux). We trained the mice to locate a clearly marked platform (visible-platform, days 1 and 2) using strategically placed visual cues. During visible-platform training, we moved the platform to a different quadrant of the pool for each session. The acquisition phase of the hidden-platform training required the mice to learn the location of the platform based on extra-maze spatial cues. In our study, we trained the mice to locate a platform that remained in the same location, and was hidden beneath opaque water (days 3–5). Mice were excluded from the study if 20% of body mass was lost over one week during treatment.

For both visible- and hidden- platform paradigms, we placed mice in the water, facing the edge of the pool, in one of nine random locations. We conducted two daily sessions, two hours apart, with each mouse. Each session consisted of three trials for which the start location changed (with 10-minute intertrial intervals). A trial ended when the mouse located the platform, and mice that failed to locate the platform within 60 seconds were led to the platform by the examiner, then forced to stay on it for 10 seconds. We removed mice that found the platform from the pool after they were on the platform for at least 3 seconds. We video-recorded the probe trials to determine distance moved using the EthoVision XT video tracking system (Noldus Information Technology), set at 6 samples/second.

To measure spatial memory retention, we conducted probe trials (platform removed) on each day of hidden-platform training, 1 hour after the last trial (i.e., three separate probe trials). For the probe trials, we placed mice into the water in the quadrant opposite the target quadrant (i.e., where the platform was previously located during hidden-platform training), and allowed the mice 60 seconds to search for the platform. We then compared the time spent in the target quadrant with the time spent in the three non-target quadrants. We also

used the average velocity and distance to the platform as a measure of performance for the visual- and hidden- platform sessions.

2.4 Molecular Assays

2.4.1 Golgi Staining and Tissue Preparation—We subjected half-brains (n = 10) to Golgi-Cox staining immediately after sacrifice. First, we immersed the samples in mercuric chloride solution for impregnation for 2 weeks, and then we immersed samples in post-impregnation buffer for 2 days. We then cut half-brains with a microtome at 200 μm in 1× phosphate-buffered saline (PBS), and put the samples into wells and washed them with 0.01 M PBS buffer (pH 7.4) with Triton X-100 (0.3%) (PBS-T). We then stained samples with ammonium hydroxide solution and immersed them in a post-staining buffer (superGolgi Kit; Bioenno Tech, LLC). Next, we washed sections in PBS-T, mounted on 1% gelatin-coated slides, and allowed them to dry. Finally, we dehydrated sections with ethanol solutions, cleaned in xylenes, and coverslipped them with Permount™ mounting medium (Fisher Scientific).

2.4.2 Spine Density and Spine Morphology—Experimenters were blinded to the experimental conditions, we conducted spine analyses on coded Golgi impregnated brain sections containing the dorsal hippocampus. We examined the spines on dendrites of the major structures of the hippocampus: dorsal ganglion (DG) granule neurons, apical (stratum radiatum), and basal (stratum oriens) dendrites of CA1and CA3 pyramidal neurons. The neurons that satisfied the following conditions were chosen for analysis in the experimental groups: presence of untruncated dendrites; consistent and dark Golgi staining along the entire extent of the dendrites; and relative isolation from neighboring neurons to avoid interference with analysis.[24] Five dendritic segments, each at least 20 μm in length,[25] were analyzed per neuron, and 6–7 neurons were analyzed per brain. We needed to establish a protocol and classification pattern to categorize the spines into general types. We chose to measure the spine-head diameter, neck diameter, and spine length, all of which are typically used by the Neurolucida software for analysis. Spine-head diameter is the maximum width of the spine head, and spine length is the distance from the tip of the spine-head to the interface with the dendritic stalk. Neurons that met staining criteria were traced using a 100 × oil objective, a computerized stage, and Neurolucida software (Ver. 11, Microbrightfield, Inc., Williston, VT).

2.4.3 Leukocyte Collection—Animals were sedated using isoflurane (5%), and we collected ~500 ul of blood from the inferior vena cava. We heparinized needles to prevent clotting. Immediately following the blood sampling, we centrifuged the blood samples, and the fraction of an anticoagulated blood sample that contained most of the white blood cells and platelets, known as the buffy coat, was isolated for analysis. We determined the number of cells via Countess™ cell counter (Fisher Scientific).

2.4.4 Dendritic Morphology Quantification—The morphological characteristics explored included Sholl analysis, total dendritic length, number of branch points, and dendritic complexity index (DCI); all performed using the Neuroexplorer component of the Neurolucida program. First, we collected the Sholl analysis, which is used to assess the

amount and distribution of the arbor at increasing distances from the cell body[26]. For our experiments, we set the distance between each radius to 20 μm. The length of dendritic branch within each progressively larger circle is counted from the soma and provided information concerning the amount and distribution of dendritic material. Next, we performed branch point analysis. A branch point represents a bifurcation of the dendrite when a branch divides into two sub-branches, and a branch point analysis is based on the number of bifurcations and the order of the points[27]. Lower branch point orders represent proximal regions of the tree, whereas larger orders characterize distal regions. The complexity of the dendritic tree is an important phenotypic component of the branching analysis, and we used the branch point analysis to determine the complexity of the dendritic arborization. We determined DCI using the following equation, DCI=Σ branch tip orders + # branch tips) × (total dendritic length/total number of primary dendrites). In the CA1, we analyzed apical and basal dendrites separately.

2.5 Data Analysis

Data were expressed as means +/− the standard error of the mean (SEM). We conducted all statistical analyses with Prism 6.0 software (GraphPad), and $P < 0.05$ was considered significant. For measures of dendritic intersections, a mixed-factors ANOVA was used to test for the effects of drug (between subjects variable) and distance from the cell body (Sholl radius, repeated measures variable), and this was followed by a Fisher least significant difference post-hoc tests when appropriate. Unpaired two-tailed t-tests with Welch's correction were used to evaluate statistical differences in platform crossings between saline and drug treated groups. Visible- and hidden-platform water maze learning curves were analyzed by two-way repeated measures ANOVA. We used Holm's correction to control for multiple comparisons, and separate analyses were conducted for the visible- and hidden-platform learning curves. For analysis of performance in the MWM probe trials, we used one-way ANOVAs with Holm's post-hoc test, when appropriate. Differences were considered to be statistically significant when $P < 0.05$.

2. RESULTS

3.1 Spatial Memory Assessment

3.1.1 Morris water maze (MWM) tests—We administered the cognitive testing using the water maze 5 weeks after chemotherapy administration. In this test, a decrease in path length (distance) to the platform indicated an improvement in spatial learning and memory. Swim velocity can influence latency to the target during training sessions. The repeated-measures ANOVA revealed there was no significant treatment-by-day interactions ($F_{(4, 80)} = 0.67$, $P = 0.61$) in the mean latency (Figure 1, Panel B). Further, all treatment groups were able to locate the visible platform (Fig. 1). Both treatment groups improved their performance, as there was a significant treatment-by day interaction, meaning mouse performance of the test improved as testing progressed which suggests that the MTX+AraC does not affect the ability of mice to perform the MWM task ($F_{(4, 64)} = 52.82$, $P < 0.001$). During the hidden-platform trials, there was no effect of MTX+AraC on memory retention ($F_{(4, 80)} = 0.67$, $P = 0.61$) (Fig. 1, **Panel B**).

3.2 Probe trials

To assess spatial memory, we administered a probe trial on training days 3–5. Saline injected animals showed spatial memory retention by spending more time in the target quadrant than the other quadrants (Fig. 2a). In contrast, animals that received MTX+AraC did not show memory retention during probe trail testing, and did not differentiate between the target and opposite quadrants ($F_{(3, 22)} = 1.23$, $P = 0.32$) (Fig 2b). The results of the spatial probe test demonstrated that compared with the sham group, MTC/AraC treated group had significantly fewer platform crossings ($P < 0.05$) (Fig. 2c)

3.3 Changes in Spine Density, Spine Morphology and Dendritic Morphology

3.3.1 Spine Density and Morphology in DG—To investigate changes in spine density and morphology, we conducted a paired t-test. Our quantitative analysis showed that after intrathecal MTX+AraC therapy, the overall spine density in the DG was unchanged (t = 0.15, p = 0.88). When we analyzed the density of different types of dendritic spines, we found that the density of thin spines was not significantly changed (t = 1.38, p = 0.21), nor was there significant change in the number of stubby spines after treatment (t = 0.79, p = 0.46). Contrastingly, there was a significant difference in the proportion of mushroom spines after treatment (t = 7.35, p < 0.0005) (Table 1).

3.3.2 Changes in Dendritic Morphology in DG—To investigate the effects of MTX +AraC treatment on neuronal morphology, a segmental Sholl analysis was performed to examine the changes in dendritic length, as a function of radial distanced from the cell soma. In the DG, there was a significant decrease in dendritic intersections after MTX+AraC from 60 to 180 μm away from the soma (Fisher's LSD, p < 0.05), indicating that the effect of treatment is associated with a different distribution of dendritic branches over the entire tree (Figure 3). Analysis also detected significant decreases in dendritic length, from 60 to 180 μm away from the soma (Fisher's LSD, p < 0.05) (Figure 3).

In addition, differences were found in total dendritic length in MTX+AraC treated animals compared to controls (t = 4.27, t < 0.05), the number of branch points (t = 13.66, p < 0.001), and branch tips (t = 9.86, p < 0.005) were also significantly decreased when compared to saline treated controls. In accordance, the dendritic complexity index of the DG, which is calculated from these parameters, was significantly different between the groups after chemotherapy (t = 8.29, p < 0.005). These data show that intrathecal MTX+AraC administration resulted in decreased dendritic complexity in the DG of mouse hippocampus (Figure 3).

3.3.3 Spine Density and Morphology in CA1—In the CA1 apical pyramidal dendrites, there were no significant changes in the overall density of spines after MTX+AraC (t = 1.03, p = 0.38). When we analyzed spine type, we found no significant changes in thin spines (t = 1.12, p = 0.35). We did find significant decreases in stubby spines (t = 3.31, p < 0.05), however; and we found significant decreases in the number of mushroom spines after treatment (t = 4.33, p <0.05). Further, MTX+AraC did not significantly decrease basal spine density (t = 0.37, p = 0.74), and there were no significant changes in thin (t = 1.95, p = 0.15) or stubby (t = 0.33, p = 0.77) spines. Yet, we saw significant decreases in the number of

mushroom spines (t = 5.43, p < 0.05) in the basal region of CA1 region of the hippocampus (Table 2).

3.3.4 Changes in Dendritic Morphology in CA1—We next performed an analysis similar to the one described in section 3.3.2 on the apical and basal regions of the CA1 pyramidal neurons. Analysis with Fisher's Least Significant Difference (LSD) showed that MTX+AraC induced alterations of apical dendrite morphology is dependent on the radial distance from the soma. Indeed, our analysis of dendritic arborization using Sholl analysis revealed that intrathecal MTX+AraC significantly decreased intersections 60–180 μm (Fisher's LSD, p<0.05) from the soma, in the apical region of CA1 (Fig. 4).

In addition, dendritic intersections were significantly decreased in the regions 40–120 μm from the soma (Fisher's LSD, p < 0.05) in the basal region of CA1. These data suggest that intrathecal chemotherapy decreased complexity at increasing distances from the soma. Similar to the observation in the DG, after MTX+AraC, differences were found in the CA1 apical and basal areas for total dendritic length (Apical t = 4.75, p < 0.05; Basal t = 5.04, p < 0.05); the number of branch points (Apical t = 5.92, p < 0.01; Basal t = 4.04, p < 0.05); and branch tips (Apical t = 5.98; Basal t = 5.10, p < 0.05). However, the branch point complexity (Apical t = 4.93, p < 0.05; Basal t = 2.03, p < 0.14) failed to reach significance (Table 2) Together, these data indicate that there was decreased dendritic complexity in the CA1 region of the hippocampus.

3.3.5 Spine Density and Morphology in CA3—Intrathecal MTX+AraC did not modulate overall density in CA 3 apical region spines (t = 2.06, p = 0.18) compared to the saline controls. Our analysis found no significant change in thin spines (t = 0.9, p = 0.46) or stubby spines (t = 1.29, p = 0.33); however, we did find significant decreases in the number of mushroom spines (t = 6.17, p <0.05) in MTX+AraC treated animals compared to controls. In the CA3 basal pyramidal dendrites, there was no significant change in the overall density of spines (t = 1.60, p = 0.25). In addition, there was no significant change in thin spines (t = 0.44, p = 0.70), stubby spines (t = 2.31, p = 0.15), or mushroom spines (t = 4.28, p = 0.0504) compared to saline treated controls (Table 3).

3.3.6 Changes in Dendritic Morphology in CA3—We performed an analysis similar to the one described in section 3.3.2 on the apical and basal regions of the CA3 pyramidal neurons. From our analysis, we found dendritic complexity had been decreased in the CA3 apical region (t = 3.33, p < 0.05) (Table 3). From Sholl analysis, we found that MTX+AraC significantly decreased CA3 apical dendritic intersections from 80–160 μm (Fisher's LSD, p<0.05). Furthermore, dendritic intersections also decreased from 60–140 μm (Fisher's LSD, p<0.05) in the CA3 basal region of the hippocampus (Fig. 5).

3.4 Decreased Peripheral Leukocytes

We observed significantly higher numbers of leukocytes after MTX+AraC treatment when compared to saline-treated controls per ml of blood (p < 0.05) (Fig. 6). Increased leukocytes could be indicative of increased systemic inflammation following chemotherapy treatment.

3. DISCUSSION

In the MWM, we observed a significant deficit in spatial memory retention in MTX/AraC-treated mice versus saline-treated controls. Saline-treated mice spent the majority of their time in the target quadrant during the probe trials, while the MTX/AraC-treated mice did not. In addition, the number of platform crossings was significantly lower in the MTX/AraC-treated group compared to the Saline treated mice. These indexes reflecting retention of memory in mice revealed that MTX/AraC treatment induced memory deficits.

Both adult and pediatric patients have demonstrated cognitive decline following chemotherapy treatment, and generally demonstrate deficits in processing speed, memory retention, executive function, and attention. These deficits extend beyond the cognitive area to physiological changes in brain matter.[28–30] Previous research demonstrated that breast cancer patients who received chemotherapy had deficits that persisted for years following treatment.[31–34] Most of the published research that studied the effects of chemotherapy on cognition limited their observations and study population to adults. Few published studies measure cognitive decline in pediatric patients, and the results of the studies that are available are often conflicting. There is evidence supporting the theory that therapy-induced cognitive decline occurs post-treatment in pediatric patients,[29,31] but other studies provide evidence to the contrary. Lofstead *et al.* published results that indicated cognitive-decline in pediatric cancer patients; the data showed decreased IQ in juvenile ALL patients exposed to chemotherapy early in life—even those who had not undergone cranial radiotherapy. Furthermore, observations from this study indicated decreased performance in verbal functioning, problem solving, spatial skills, attention, and processing speed for the pediatric patients treated with modern ALL treatment protocols.[35] Von der Weid *et al.* found contradictory data and reported in 2003 that pediatric ALL patients treated with chemotherapy-only regimens showed normal and comparable intellectual performance to those surviving from non-CNS tumors.[36] Furthermore, several animal studies have reported that various anticancer agents impair cognitive performance in cancer-free rodents. Juvenile mice were given intraperitoneal (IP) injections of MTX, AraC, or MTX+AraC (injections given post-natal day 14). This study found animals that received MTX to be cognitively impaired during behavior tasks. Animals that received high doses of MTX and MTX in combination with AraC showed the highest instance of deficit in behavioral tasks.[20]

These results were consistent with clinical findings that childhood cancer survivors experience impairments in learning new information and exhibit deficits years after chemotherapy. In another study, adult mice were given IP injections of MTX, and hippocampi were extracted. At 1 and 7 days post injections, mice underwent an open field test, novel object recognition (NOR) task, and tail suspension test. Data showed that mice treated with MTX were behaviorally impaired and demonstrated cognitive impairment and depression-like behavior. In addition, hippocampal cells showed reduced proliferating cells and immature progenitor neurons. Previously, MTX was shown to induce apoptosis in cultured immature hippocampal cells, but not in mature hippocampal cells.[37] Another study found that IP injections of MTX led to hippocampal dysfunction and cognitive impairment and depressive-like behaviors.[38] Literature reporting data results from tests that measure

cognitive decline in juvenile mice is lacking, and more studies, like this one, are necessary to investigate possible mechanisms that lead to cognitive decline in pediatric populations.

The findings of our study are congruent with the few published manuscripts available in the literature that demonstrate cognitive decline following treatment with MTX and/or AraC in pediatric or juvenile populations. Bisen-Hersh *et al.* demonstrated that IP chemotherapy treatment in juvenile mice led to decreased memory retention in behavioral tasks. In their study, mice completed a NOR task and an autoshaping task. In both tests, mice that received chemotherapy did not score as well in memory retention compared to controls.[20] However, MTX and AraC are usually given in combination in an intrathecal injection.[7] Previous studies have not examined the effects of intrathecal therapy in learning and memory. Our study uses intrathecal injections to adhere more closely to the treatment protocols in pediatric human patients with ALL.

Further, changes in hippocampal dendrites and dendritic spine morphology play a major role in the formation and consolidation of memories. Excitatory synapses are located on dendritic arms and are responsible for the process of learning and memory. Prolonged excitation at these synapses leads to changes in dendritic spine morphology and are the basis of physiological and cellular properties of memory consolidation.[39–44] Exposure to toxic materials in this area results in retraction and remodeling of dendrites, which can greatly affect the process of memory consolidation.[39–41] Other studies have observed similar learning impairments and decreased memory capabilities in animals exposed to chemotherapy. Andres *et a*l. determined that dendritic arborization was significantly decreased in hippocampal neurons of the CA1 and CA3 regions of the hippocampus after exposure to cisplatin chemotherapy. In this study, cisplatin also led to reduction in neuronal stem cells in the dentate gyrus of the hippocampus.[39] Another study found that cisplatin treatment decreased arborization but dendritic spine density was also altered in hippocampal regions.[45] Our lab has previously demonstrated similar changes in dendritic morphology after chemotherapy treatment in aged mice that received 5-fluorouracil (5-Fu) treatment. In this study, animals that received 5-Fu were memory impaired, and changes in performance during behavioral tasks coincided with reductions in dendrite morphology.[46]

Data from the current study is consistent with previous findings. In our study, we observed decreased dendritic arborization as well as changes in spine morphology that correspond with memory deficits. However, our study is the first, to our knowledge, to demonstrate behavioral evidence of cognitive decline in parallel with histological changes following chemotherapy treatment in a juvenile murine model. Since chemotherapy exposure in juveniles occurs at acritical time in development, investigation of this type of cognitive decline must be explored and potentially ameliorated. In addition, we found changes in dendritic complexity and spine density across the dentate gyrus, CA1 and CA3 regions of the hippocampus (Fig. 5, above). Other studies have also reported similar differences across brain regions. The hippocampal CA3 region has previously been associated with sequential associations of memories, while the CA1 region has been associated with the retrieval of memories with temporal context.[41] This could potentially provide explanation of greater changes in the CA1 region after intrathecal MTX+AraC than in the CA3. In the MWM, we saw decreased spatial memory retention in MTX+AraC treated animals when compared to

controls. The cause of the decreased memory in the MWM could be an inability to recall or retrieve these spatial memories in chemotherapy treated animals.

Another common complication of intrathecal of chemotherapy treatment with MTX and AraC is leukoencephalopathy.[5] Neuroinflammation has previously been proposed as a possible mechanism that contributes to cognitive decline following chemotherapy treatment.[47,48] Intrathecal drug administration ensures CNS exposure to MTX and AraC. The induction of an inflammatory response in the CNS could lead to activation of microglia. Neuroinflammation may to lead to synaptic damage and neurodegeneration. Inflammatory cytokines released from activated microglia leads to neurotoxicity and could be responsible for decreases in cognitive function.[49] In figure 6, we demonstrate that circulating leukocytes were significantly increased in mice treated with intrathecal MTX+AraC compared to the saline treated controls. This could be indicative of an overall state of inflammation. It has previously been determined that activated leukocytes are able to cross the blood brain barrier.[50] If there are increased circulating leukocytes after chemotherapy treatment, there could be higher numbers of activated leukocytes in the CNS, which would contribute to neuroinflammation by inducing microglia activation, due to the presence of cytokines secreted from these leukocytes significantly (* $p < 0.05$).

In conclusion, cognitive decline following intrathecal chemotherapy can greatly affect the quality of life of ALL patients for years after the cessation of treatment. Many juvenile patients experience decreased learning, attention, and memory following modern treatment protocols. Underlying mechanisms of cognitive decline remain elusive. It is imperative that studies determine the underlying mechanisms that contribute to this type of cognitive decline as ameliorative strategies and interventions could potentially increase patient success and quality of life. Future studies should address potential mechanisms that could lead to cognitive decline, such as neuroinflammation, oxidative stress, and changes in vascularization, all of which have been implicated in cognitive decline. Understanding the pathophysiological changes of cognitive decline would allow for the development of better treatment protocols and improve patient care.

Acknowledgments

Funding source: This work was supported by Pilot Grant under NIH P20 GM109005 (ARA).

This manuscript was edited by Madison Hedrick, MA, of the Science Communication Group at the University of Arkansas for Medical Sciences.

References

1. Reiter A, et al. Chemotherapy in 998 unselected childhood acute lymphoblastic leukemia patients. Results and conclusions of the multicenter trial ALL-BFM 86. Blood. 1994; 84:3122–3133. [PubMed: 7949185]
2. Veerman AJ, et al. High cure rate with a moderately intensive treatment regimen in non-high-risk childhood acute lymphoblastic leukemia. Results of protocol ALL VI from the Dutch Childhood Leukemia Study Group. Journal of clinical oncology : official journal of the American Society of Clinical Oncology. 1996; 14:911–918. DOI: 10.1200/JCO.1996.14.3.911 [PubMed: 8622039]

3. Group, C. A. C. Duration and intensity of maintenance chemotherapy in acute lymphoblastic leukaemia: overview of 42 trials involving 12 000 randomised children. The Lancet. 1996; 347:1783–1788.

4. van Dongen JJ, et al. Prognostic value of minimal residual disease in acute lymphoblastic leukaemia in childhood. The Lancet. 1998; 352:1731–1738.

5. Bhojwani D, Yang JJ, Pui C-H. Biology of childhood acute lymphoblastic leukemia. Pediatric clinics of North America. 2015; 62:47–60. [PubMed: 25435111]

6. Cooper SL, Brown PA. Treatment of pediatric acute lymphoblastic leukemia. Pediatric clinics of North America. 2015; 62:61–73. DOI: 10.1016/j.pcl.2014.09.006 [PubMed: 25435112]

7. Pieters R, Carroll WL. Biology and treatment of acute lymphoblastic leukemia. Hematology/oncology clinics of North America. 2010; 24:1–18. DOI: 10.1016/j.hoc.2009.11.014 [PubMed: 20113893]

8. Shuper A, et al. Methotrexate-related neurotoxicity in the treatment of childhood acute lymphoblastic leukemia. The Israel Medical Association journal : IMAJ. 2002; 4:1050–1053. [PubMed: 12489505]

9. Bhojwani D, et al. Methotrexate-induced neurotoxicity and leukoencephalopathy in childhood acute lymphoblastic leukemia. Journal of Clinical Oncology. 2014; 32:949–959. [PubMed: 24550419]

10. Tannock IF, Ahles TA, Ganz PA, Van Dam FS. Cognitive impairment associated with chemotherapy for cancer: report of a workshop. Journal of Clinical Oncology. 2004; 22:2233–2239. [PubMed: 15169812]

11. Kim JH, Kim SH, Eidinoff ML. Cell viability and nucleic acid metabolism after exposure of HeLa cells to excess thymidine and deoxyadenosine. Biochemical pharmacology. 1965; 14:1821–1829. [PubMed: 5880537]

12. Talley RW, O'Bryan RM, Tucker WG, Loo RV. Clinical pharmacology and human antitumor activity of cytosine arabinoside. Cancer. 1967; 20:809–816. [PubMed: 6071587]

13. Marsh JC. The effects of cancer chemotherapeutic agents on normal hematopoietic precursor cells: a review. Cancer research. 1976; 36:1853–1882. [PubMed: 773531]

14. Baker WJ, Royer GL Jr, Weiss RB. Cytarabine and neurologic toxicity. Journal of clinical oncology : official journal of the American Society of Clinical Oncology. 1991; 9:679–693. DOI: 10.1200/JCO.1991.9.4.679 [PubMed: 1648599]

15. Moore HC. An overview of chemotherapy-related cognitive dysfunction, or 'chemobrain'. Oncology. 2014; 28:797–804. [PubMed: 25224480]

16. Argyriou AA, Assimakopoulos K, Iconomou G, Giannakopoulou F, Kalofonos HP. Either called "chemobrain" or "chemofog," the long-term chemotherapy-induced cognitive decline in cancer survivors is real. Journal of pain and symptom management. 2011; 41:126–139. DOI: 10.1016/j.jpainsymman.2010.04.021 [PubMed: 20832978]

17. Kesler SR, Tanaka H, Koovakkattu D. Cognitive reserve and brain volumes in pediatric acute lymphoblastic leukemia. Brain imaging and behavior. 2010; 4:256–269. [PubMed: 20814845]

18. Eiser C. Cognitive deficits in children treated for leukaemia. Archives of disease in childhood. 1991; 66:164. [PubMed: 1899787]

19. Askins MA, Moore BD 3rd. Preventing neurocognitive late effects in childhood cancer survivors. Journal of child neurology. 2008; 23:1160–1171. DOI: 10.1177/0883073808321065 [PubMed: 18952582]

20. Bisen-Hersh EB, Hineline PN, Walker EA. Effects of early chemotherapeutic treatment on learning in adolescent mice: implications for cognitive impairment and remediation in childhood cancer survivors. Clinical cancer research : an official journal of the American Association for Cancer Research. 2013; 19:3008–3018. DOI: 10.1158/1078-0432.CCR-12-3764 [PubMed: 23596103]

21. Bourne JN, Harris KM. Balancing structure and function at hippocampal dendritic spines. Annual review of neuroscience. 2008; 31:47–67. DOI: 10.1146/annurev.neuro.31.060407.125646

22. Mateos JM, et al. Synaptic modifications at the CA3–CA1 synapse after chronic AMPA receptor blockade in rat hippocampal slices. The Journal of physiology. 2007; 581:129–138. [PubMed: 17303644]

23. Jarrard LE. What does the hippocampus really do? Behavioural brain research. 1995; 71:1–10. [PubMed: 8747170]

24. Titus AD, et al. Hypobaric hypoxia-induced dendritic atrophy of hippocampal neurons is associated with cognitive impairment in adult rats. Neuroscience. 2007; 145:265–278. DOI: 10.1016/j.neuroscience.2006.11.037 [PubMed: 17222983]
25. Magarinos AM, et al. Effect of brain-derived neurotrophic factor haploinsufficiency on stress-induced remodeling of hippocampal neurons. Hippocampus. 2011; 21:253–264. DOI: 10.1002/hipo.20744 [PubMed: 20095008]
26. Sholl DA. Dendritic organization in the neurons of the visual and motor cortices of the cat. J Anat. 1953; 87:387–406. [PubMed: 13117757]
27. Morley BJ, Mervis RF. Dendritic spine alterations in the hippocampus and parietal cortex of alpha7 nicotinic acetylcholine receptor knockout mice. Neuroscience. 2013; 233:54–63. DOI: 10.1016/j.neuroscience.2012.12.025 [PubMed: 23270857]
28. Simo M, Rifa-Ros X, Rodriguez-Fornells A, Bruna J. Chemobrain: a systematic review of structural and functional neuroimaging studies. Neuroscience and biobehavioral reviews. 2013; 37:1311–1321. DOI: 10.1016/j.neubiorev.2013.04.015 [PubMed: 23660455]
29. Simo M, et al. Cognitive and brain structural changes in a lung cancer population. Journal of thoracic oncology : official publication of the International Association for the Study of Lung Cancer. 2015; 10:38–45. DOI: 10.1097/JTO.0000000000000345
30. Lepage C, et al. A prospective study of grey matter and cognitive function alterations in chemotherapy-treated breast cancer patients. SpringerPlus. 2014; 3:444. [PubMed: 25184110]
31. Jim HS, et al. Meta-analysis of cognitive functioning in breast cancer survivors previously treated with standard-dose chemotherapy. Journal of Clinical Oncology. 2012; 30:3578–3587. [PubMed: 22927526]
32. Taillibert S, Le Rhun E, Chamberlain MC. Chemotherapy-Related Neurotoxicity. Current neurology and neuroscience reports. 2016; 16:81. [PubMed: 27443648]
33. Bower, JE., Ganz, PA. Improving Outcomes for Breast Cancer Survivors. Springer; 2015. p. 53-75.
34. Lacourt TE, Heijnen CJ. Mechanisms of Neurotoxic Symptoms as a Result of Breast Cancer and Its Treatment: Considerations on the Contribution of Stress, Inflammation, and Cellular Bioenergetics. Current Breast Cancer Reports. 2017; 9:70–81. [PubMed: 28616125]
35. Lofstad GE, Reinfjell T, Hestad K, Diseth TH. Cognitive outcome in children and adolescents treated for acute lymphoblastic leukaemia with chemotherapy only. Acta paediatrica. 2009; 98:180–186. [PubMed: 18826490]
36. Von der Weid N, et al. Intellectual outcome in children and adolescents with acute lymphoblastic leukaemia treated with chemotherapy alone: age-and sex-related differences. European Journal of Cancer. 2003; 39:359–365. [PubMed: 12565989]
37. Yang M, et al. Neurotoxicity of methotrexate to hippocampal cells in vivo and in vitro. Biochemical pharmacology. 2011; 82:72–80. [PubMed: 21459079]
38. Yang M, et al. Acute treatment with methotrexate induces hippocampal dysfunction in a mouse model of breast cancer. Brain research bulletin. 2012; 89:50–56. [PubMed: 22796103]
39. Andres AL, Gong X, Di K, Bota DA. Low-doses of cisplatin injure hippocampal synapses: a mechanism for 'chemo' brain? Experimental neurology. 2014; 255:137–144. DOI: 10.1016/j.expneurol.2014.02.020 [PubMed: 24594220]
40. Avila-Costa MR, et al. Hippocampal cell alterations induced by the inhalation of vanadium pentoxide (V 2 O 5) promote memory deterioration. Neurotoxicology. 2006; 27:1007–1012. [PubMed: 16684564]
41. Sheng M, Hoogenraad CC. The postsynaptic architecture of excitatory synapses: a more quantitative view. Annu. Rev. Biochem. 2007; 76:823–847. [PubMed: 17243894]
42. Kasai H, Fukuda M, Watanabe S, Hayashi-Takagi A, Noguchi J. Structural dynamics of dendritic spines in memory and cognition. Trends in neurosciences. 2010; 33:121–129. [PubMed: 20138375]
43. Martin SJ, Grimwood PD, Morris RG. Synaptic plasticity and memory: an evaluation of the hypothesis. Annual review of neuroscience. 2000; 23:649–711.
44. Neves G, Cooke SF, Bliss TV. Synaptic plasticity, memory and the hippocampus: a neural network approach to causality. Nature reviews. Neuroscience. 2008; 9:65. [PubMed: 18094707]

45. Zhou W, Kavelaars A, Heijnen CJ. Metformin prevents cisplatin-induced cognitive impairment and brain damage in mice. PloS one. 2016; 11:e0151890. [PubMed: 27018597]

46. Groves TR, et al. 5-Fluorouracil chemotherapy upregulates cytokines and alters hippocampal dendritic complexity in aged mice. Behavioural brain research. 2017; 316:215–224. [PubMed: 27599618]

47. Myers JS. The possible role of cytokines in chemotherapy-induced cognitive deficits. Advances in experimental medicine and biology. 2010; 678:119–123. [PubMed: 20738013]

48. Myers JS, Pierce J, Pazdernik T. Oncology nursing forum.

49. Kraft AD, Harry GJ. Features of microglia and neuroinflammation relevant to environmental exposure and neurotoxicity. International journal of environmental research and public health. 2011; 8:2980–3018. [PubMed: 21845170]

50. Takeshita Y, Ransohoff RM. Inflammatory cell trafficking across the blood–brain barrier: chemokine regulation and in vitro models. Immunological reviews. 2012; 248:228–239. [PubMed: 22725965]

Highlights

- MTX/AraC significantly compromised the dendritic architecture.
- MTX/AraC modulated spine morphology throughout Hippocampus.
- MTX/AraC impaired hippocampal dependent Behavior

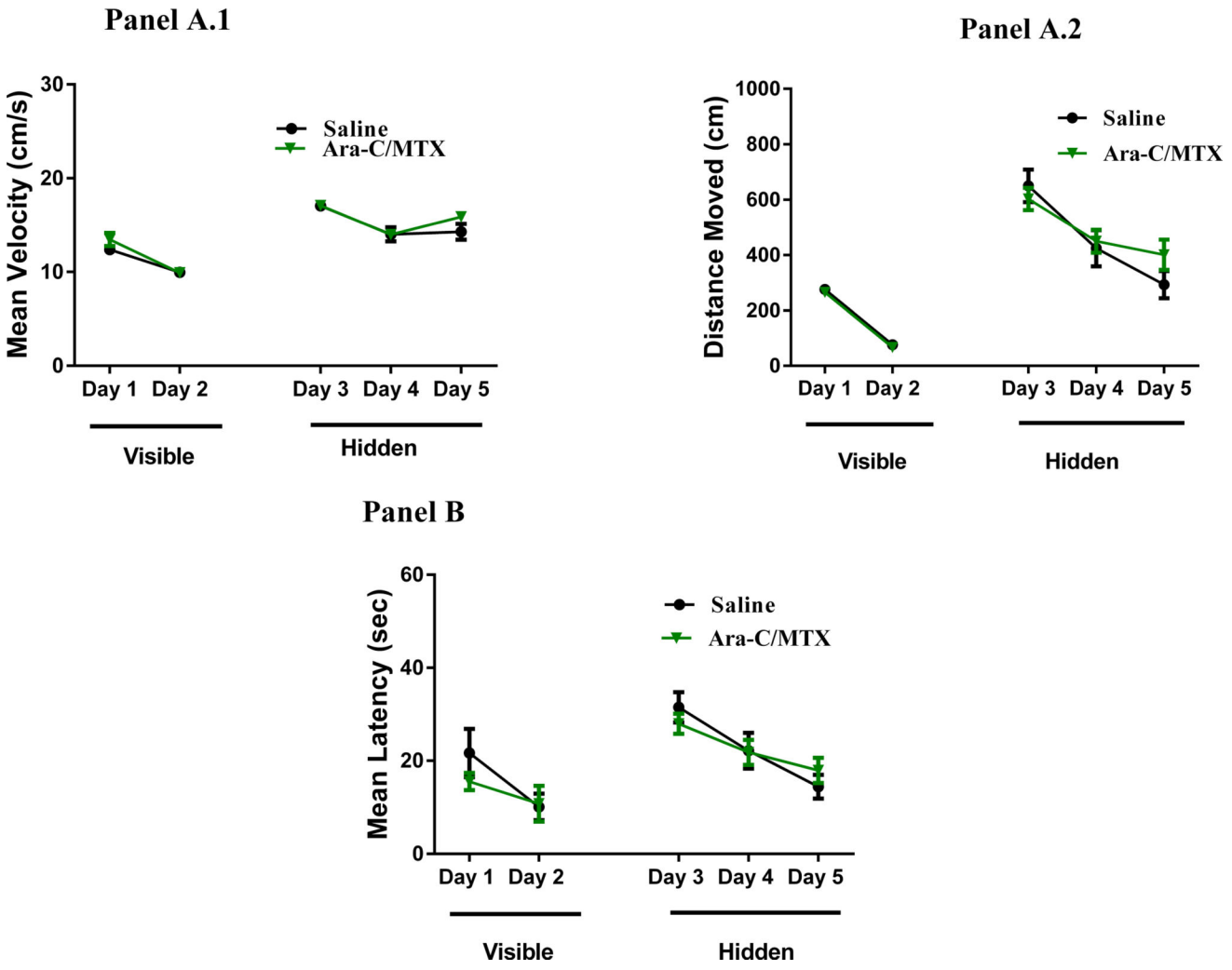

Figure 1.

Distances moved to the target platform during visible- and hidden-platform training sessions. Panel A*1*: There were no significant group differences in velocity during the visible- or hidden-platform training. Panel A2: During the visible-platform training (days 1 and 2), all experimental groups swam similar distances to the platform. Panel B: All groups showed daily improvements in their ability to locate during the hidden-platform training (days 3–5).

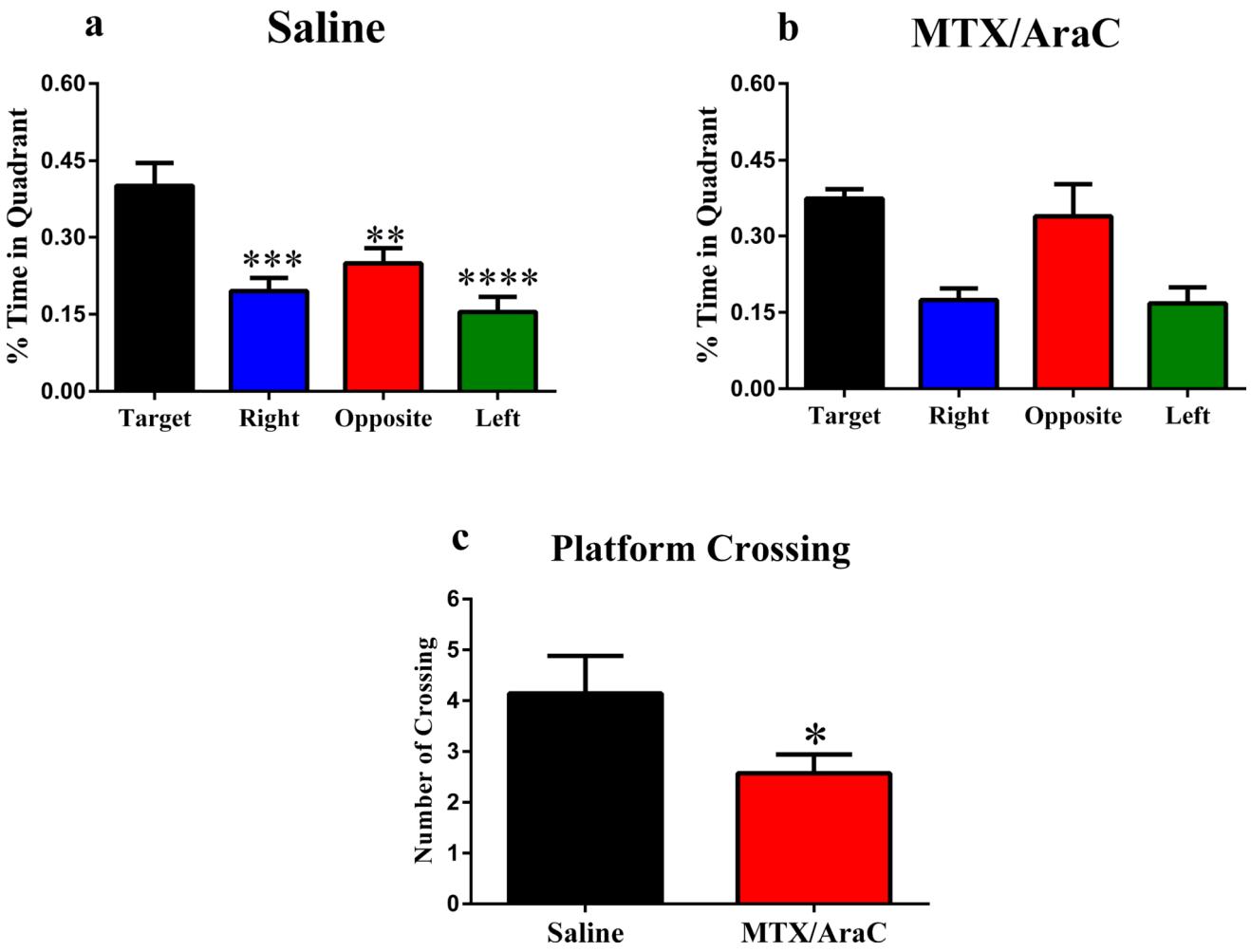

Figure 2.

Spatial memory retention in mice during the Morris water maze probe trial, after the first day of hidden-platform training. Panels A: Animals that received saline injections showed memory retention and spent significantly more time in the target quadrant ($P < 0.05$). Panel B: Animals that received MTX+AraC injections did not show memory retention during testing. Panel C: After removal of the platform on day 3, the number of platform crossings. Each bar represents the mean of 8–10 mice; error bars are SEM.

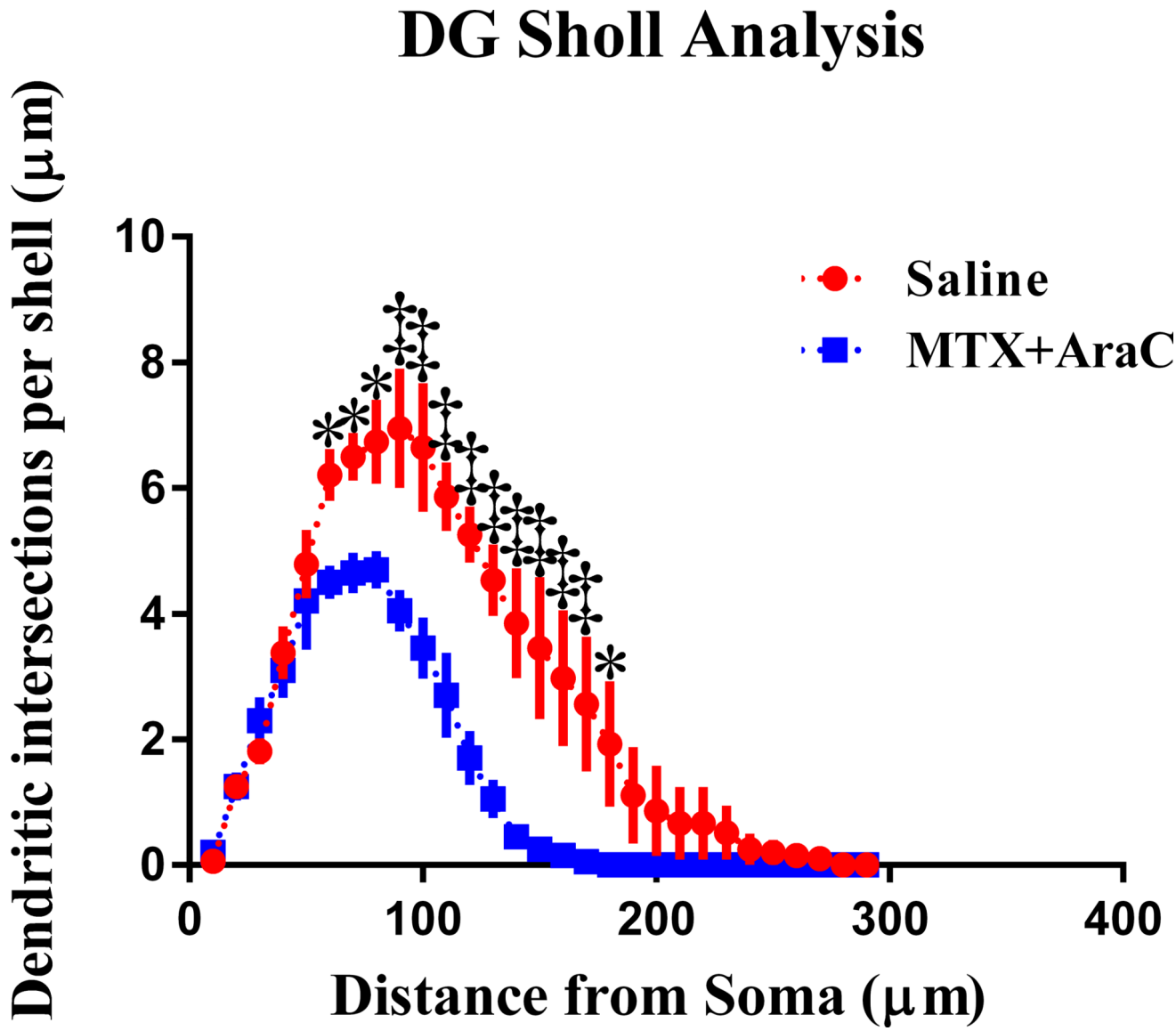

FIG. 3.

Sholl analyses and dendrite complexity of DG neurons. Dendritic intersections measured by Sholl analysis revealed a decrease in arborization that was particularly evident after exposure to MTX/AraC at 60–180 µm away from the soma. Average ± SEM (n = 6); * $P < 0.01$; ‡ $P < 0.001$.

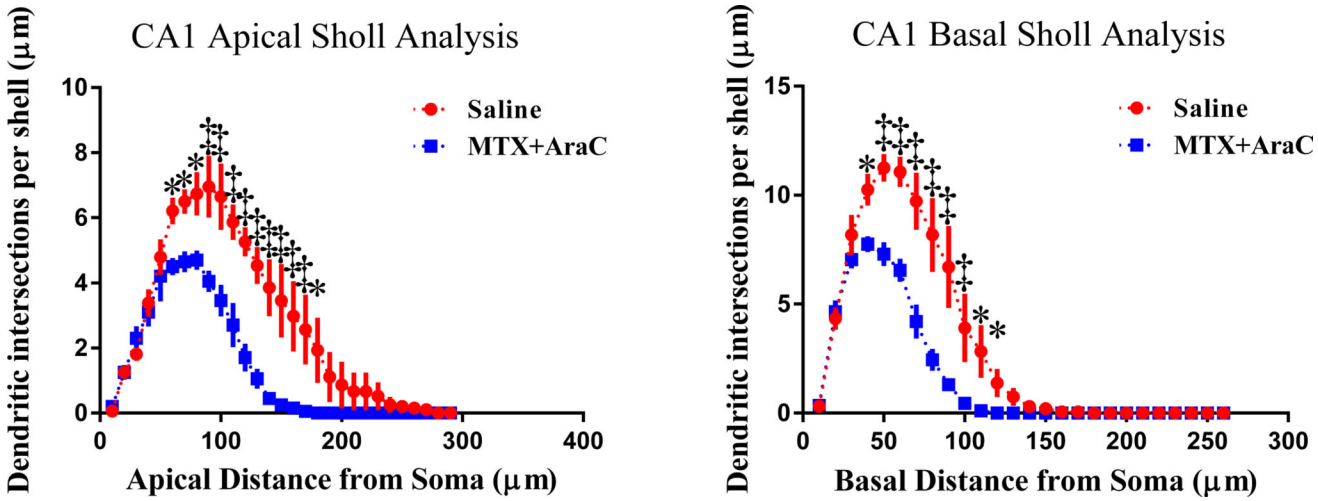

FIG. 4.

Sholl analysis of CA1 apical and basal pyramidal neurons. Left Panel: Sholl analysis revealed that MTX/AraC significantly decreased arborization in CA1 apical pyramidal dendrites at a distance of 60–180 μm from the soma. Right Panel: MTX/AraC decreased arborization at a distance of 40–120 μm from the soma. Average ± SEM (n = 6) * $P < 0.01$; ‡ $P < 0.0001$.

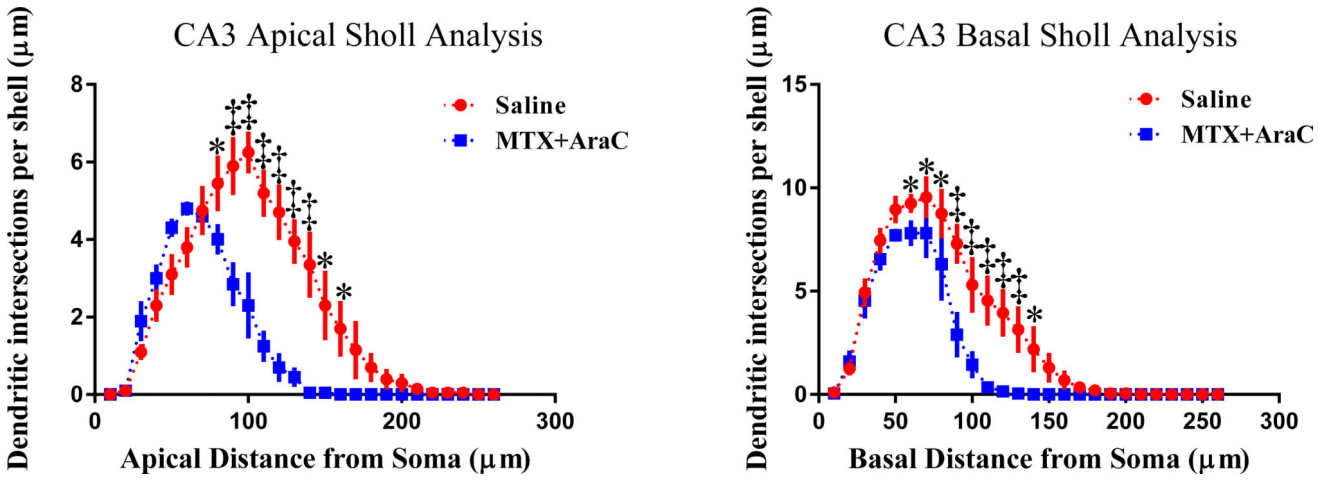

FIG. 5.

Sholl analysis of CA3 apical and basal pyramidal neurons. Left Panel: Sholl analysis revealed that MTX/AraC significantly decreased arborization in CA3 apical pyramidal dendrites at a distance of 80–160 µm from the soma. Panel B: MTX/AraC significantly decreased arborization at distances of 60–140 µm from the soma in CA3 basal pyramidal dendrites. Average ± SEM (n = 6); * $P < 0.05$; ‡ $P < 0.001$.

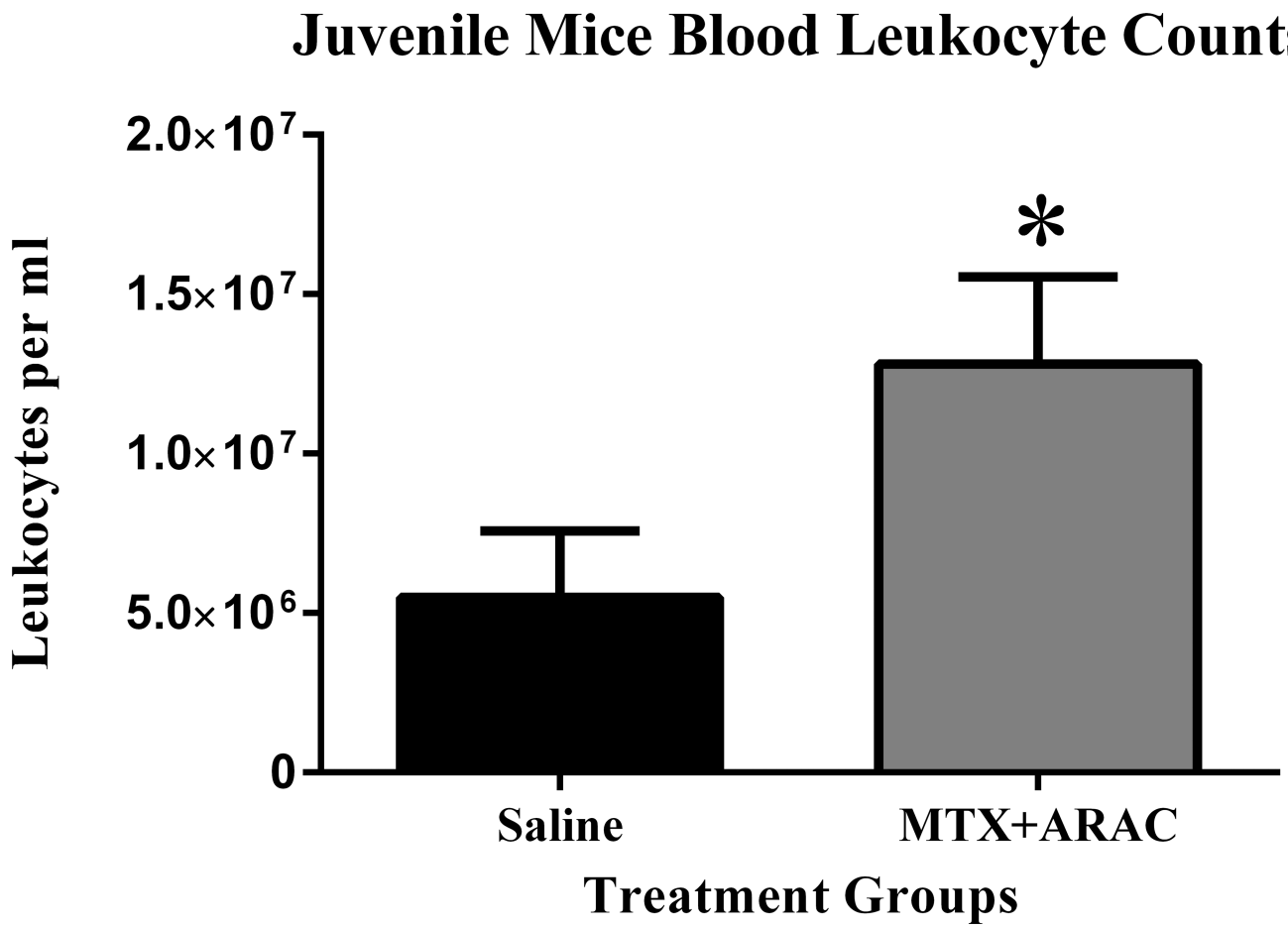

FIG. 6.

Circulating leukocyte counts, 3 months-post MTX+AraC administration. After MTX+AraC exposure, the number of circulating leukocytes per ml of blood increased. * $p < 0.05$.

Author Manuscript

Author Manuscript

Author Manuscript

TABLE 1

Effects of MTX+AraC on Spine Morphology in Hippocampal DG

Cell types and measurements	Saline[a]	MTX+AraC[a]	*P* value
Thin spines (no.)	53.74 ± 2.22	57.04 ± 1.71	P = 0.21
Stubby spines (no.)	33.07 ± 2.08	36.38 ± 1.54	P = 0.46
Mushroom spines (no.)	13.19 ± 0.39	6.58 ± 0.60	**P < 0.0001**[b]
Overall density (no.)	20.84 ± 0.38	20.81 ± 0.49	P = 0.87
Total dendritic length (μm)	1277 ± 58.07	721 ± 56.39	**P < 0.05**
Total branch points (no.)	12.55 ± 0.26	5.54 ± 0.34	**P < 0.001**
Total branch tips (no.)	14.00 ±0.18	7.15 ± 0.53	**P < 0.005**
Dendritic complexity	67345 ± 7543	11523 ± 1236	**P < 0.005**

[a]Mean ± SEM.

[b]Values in boldface are significant.

TABLE 2

Morphological Analysis of Apical and Basal Dendrites in CA1

Cell types and measurements	Saline[a]	MTX+AraC[a]	*P* value
CA1 apical			
Thin spines (no.)	53.3 ± 0.92	54.55 ±2.27	P = 0.35
Stubby spines (no.)	33.64 ± 1.18	38.39 ± 1.17	**P < 0.05**[b]
Mushroom spines (no.)	13.06 ± 2.29	7.06 ± 1.22	**P < 0.01**
Overall density (no.)	21.89 ± 0.75	20.15 ± 0.68	P = 0.38
Total dendritic length (μm)	1114 ± 91.97	555.4 ±22.06	**P < 0.05**
Total branch points (no.)	12.9 ±1.76	7.10 ± 0.50	**P < 0.05**
Total branch tips (no.)	12.93 ± 0.88	8.05 ± 0.29	**P <0.01**
Dendritic complexity	101280 ± 13090	23027 ± 2254	**P < 0.05**
CA1 basal			
Thin spines (no.)	50.44 ± 2.74	54.36 ±1.25	P = 0.15
Stubby spines (no.)	36.39 ±2.77	38.59 ± 0.52	P = 0.77
Mushroom spines (no.)	13.18 ±0.42	7.05 ± 0.98	**P < 0.001**
Overall density (no.)	19.48 ±0.39	19.31 ± 0.44	P 0.74
Total dendritic length (μm)	1127 ± 76.95	588 ± 25.95	**P < 0.05**
Total branch points (no.)	13.25 ± 1.3	6.35 ± 0.66	**P < 0.05**
Total branch tips (no.)	15.39 ± 0.69	9.45 ± 0.40	**P < 0.05**
Dendritic complexity	38711 ± 15619	5847 ± 1113	**P < 0.005**

[a] Mean ± SEM.

[b] Values in boldface are significant.

TABLE 3

Morphological Analysis of Apical and Basal Dendrites in CA3

Cell types and measurements	Saline[a]	MTX+AraC[a]	*P* value
CA3 apical			
Thin spines (no.)	53.21 ± 1.89	54.87 ± 3.75	p = 0.46
Stubby spines (no.)	34.74 ± 1.20	37.6 ± 3.93	p = 0.33
Mushroom spines (no.)	12.06 ±1.04	7.59 ± 0.24	p = 0.05
Overall density (no.)	20.18 ± 0.28	20.90 ± 0.77	p = 0.18
Total dendritic length (μm)	844.9 ± 50.72	557.2 ± 63.10	p = 0.11
Total branch points (no.)	7.68 ± 0.26	6.75 ± 0.63	p = 0.39
Total branch tips (no.)	9.08 ± 0.32	8.45 ± 0.86	p = 0.69
Dendritic complexity	29209 ± 3570	13227 ± 1951	**p < 0.05**
CA3 basal			
Thin spines (no.)	51.39 ± 1.35	50.11 ± 1.62	p = 0.70
Stubby spines (no.)	36.64 ± 0.81	41.06 ± 0.87	p = 0.15
Mushroom spines (no.)	11.97 ± 0.76	8.84 ± 0.82	**p < 0.05**
Overall density (no.)	20.51 ± 0.25	19.63 ± 0.95	p = 0.25
Total dendritic length (μm)	1200 ± 96.61	777.3 ± 81.67	p = 0.35
Total branch points (no.)	10.48 ± 0.71	8.35 ± 0.70	p = 0.35
Total branch tips (no.)	13.68 ± 0.87	11.60 ± 0.58	p = 0.29
Dendritic complexity	24122 ± 5107	11890 ± 2978	**p < 0.05**

[a]Mean ± SEM.

[b]Values in boldface are significant.